Ocean Systems Engineering, *Vol. 6, No. 2 (2016) 129-141*
DOI: http://dx.doi.org/10.12989/ose.2016.6.2.129

Analytical and numerical analysis for unbonded flexible risers under axisymmetric loads

Yousong Guo[*1], Xiqia Chen[2] and Deyu Wang[1]

[1]State Key Laboratory of Ocean Engineering, Shanghai Jiao Tong University, 800 Dongchuan Road, Min Hang, Shanghai, China
[2]Tianjin Branch, CNOOC Ltd, Tianjin, China

(Received March 2, 2016, Revised May 3, 2016, Accepted May 10, 2016)

Abstract. Due to the structural complexity, the response of a flexible riser under axisymmetric loads is quite difficult to determine. Based on equilibrium conditions, geometrical relations and constitutive equations, an analytical model that can accurately predict the axisymmetric behavior of flexible risers is deduced in this paper. Since the mutual exclusion between the contact pressure and interlayer gap is considered in this model, the influence of the load direction on the structural behavior can be analyzed. Meanwhile, a detailed finite element analysis for unbonded flexible risers is conducted. Based on the analytical and numerical models, the structural response of a typical flexible riser under tension, torsion, internal and outer pressure has been studied in detail. The results are compared with experimental data obtained from the literature, and good agreement is found. Studies have shown that the proposed analytical and numerical models can provide an insightful reference for analysis and design of flexible risers.

Keywords: flexible riser; axisymmetric response; analytical model; numerical model; gap between the layers

1. Introduction

As the exploitation of the oil-gas resource advances into deeper waters and harsher environment, flexible risers are more and more widely used, serving as the essential channel transiting oil-gas from the wellhead to the offshore rig (Do 2011, Huang *et al*. 2013, Zou 2011). The main advantage of flexible risers is that they are compliant and highly deformable in bending, while maintaining enough tensile stiffness to enable them to undergo large deformations induced by currents, waves, vortex-induced vibrations, and the motion of floating vessels. However, due to their elaborate structure, the design and analysis of flexible risers is a complex and difficult topic.

Because of their importance in the offshore industry, unbonded flexible risers have been the subject of intensive research in last 15 years. Among the analytical works, Feret and Bournazel (1987) analyzed the behavior of high-pressure unbonded flexible risers. They derived simple formulas for the stresses and the contact pressures between layers in flexible risers under axisymmetrical loads. Witz and Tan (1992) proposed an analytical nonlinear model for predicting

∗Corresponding author, Ph.D., E-mail: guoyousong@sjtu.edu.cn

http://www.techno-press.org/?journal=ose&subpage=7 ISSN: 2093-6702 (Print), 2093-677X (Online)

load-displacement relationship, interfacial contact pressures and interlayer gap amplitudes of flexible risers under axisymmetrical loads. The model treated the flexible risers as a combination of helical and cylindrical components, the cylindrical layers were considered as long thin-walled cylinders and the helical armors were governed by Love's equilibrium equations. Ramos Jr. and Pesce (2004) proposed a more advanced analytical model by considering geometric and contact nonlinearities in the structural analysis of flexible risers. Using sets of equations, which comprises equilibrium conditions, constitutive equations and geometrical relations, this model presented a consistent and comprehensive solution in terms of stresses and deformations for the flexible riser subjected to combined loads. Saevik and Bruaseth (2005) presented a finite element formulation for predicting the structural behavior of umbilical cables by combining curved beam kinematics, thin shell theory and the principle of virtual displacements. The formulation took into account a number of features, such as material non-linearity, gap between individual bodies, and hoop response due to contact effects.

The mechanical behavior of unbonded flexible risers is highly nonlinear because of the structural complexity. Hence, the analytical models mentioned above are quite complicated and their range of applicability is limited by the simplified assumptions on which they are based. This has motivated a significant amount of research into the development of refined finite element models. In particular, Zhang and Tuohy (2002) studied the application of finite-element model to structural analysis of unbonded flexible risers using the ANSYS software. They used elements with equivalent material and geometric properties to model contact between layers. They suggested taking friction at the contact surface into account and using 3D solid elements in modeling. Bahtui *et al*. (2008a,b) studied the response of a five-layer flexible riser under axisymmetric loads with a detailed three-dimensional finite-element model using the ABAQUS software. In this model, all layers were represented by 3D solid elements and contact elements, with friction properties defined between each contact pair of layers. According to the authors, very good agreement between the proposed and analytical models (Claydon *et al*. 1992, Mcnamara and Harte 1989, Lanteigne 1985) was found.

For the experimental work, a case study involving the structural analysis of a 2.5-inch flexible riser was of crucial importance (Witz 1996). In this case, the axial and torsional stiffness under different boundary conditions were experimentally evaluated. The author described the internal layers of the riser in detail and proposed a "blind" test to several institutions by asking them to estimate the stiffness with their models. Generally, the results provided by the institutions agreed well with the experimental ones for the tensional and torsional response of the riser.

Based on research work done previously, the research presented in this paper has combined analytical work with the numerical one to obtain deep insights into the structural behavior. In this paper, an analytical model to predict the behavior of the flexible riser under axisymmetric loads is presented. Meanwhile, a very detailed finite element model is developed in ABAQUS software. Based on the developed analytical model and finite element model, the structural behavior of the flexible riser under tension, torque, internal and outer pressure is investigated. The results are compared with experimental data obtained from the literature, and good agreements are obtained.

2. Analytical model

A typical flexible riser is shown in Fig. 1. The components of a flexible riser can be divided into two parts: helical layers and cylindrical layers. To study structural response of a flexible layer with n helical layers and m polymeric layers, the number of the variables is listed in Table 1. In this table, index *i* represented the number of the layer, ranging from 1 (innermost layer) to n+m (outermost layer).

Because of the non-bonded connections between each layer, the variables of $p_{c,i}$ and g_i is mutually exclusive, i.e., if $p_{c,i} \neq 0$, then $g_i = 0$; while if $g_i \neq 0$, then $p_{c,i} = 0$. This special structural characteristic leads to different structural response of flexible risers under different direction loads.

In this paper the analytical model is deducted based on equilibrium conditions, geometrical relations and constitutive equations. All the deductions and analysis are based on the assumptions below

1). In each layer, the ratio of axial elongation ($\Delta\mu / L$) and torsional curvature ($\Delta\phi / L$) are identical and infinetsmal;
2). No interlayer gap exists before deformation;
3). The material of each layer is linear elastic;
4). The variance in radius and thickness of each layer are uniform.

Considering the structural composition of a flexible riser, the following analysis is carried out in terms of helical layers and cylindrical layers separately.

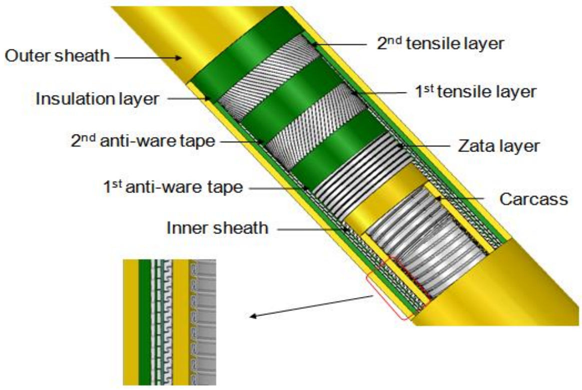

Fig. 1 Schematic diagram of a typical flexible riser

Table 1 Variables related to the problem

Unknown variables	quantity
Interlayer pressure ($p_{c,i}$) (or interlayer gap (g_i))	n+m-1
Axial force of the ith layer (F_i)	n+m
Torque of the ith layer (M_i)	n+m
Radial displacement of the ith layer (Δr_i)	n+m
Variance in thickness of the ith layer (Δt_i)	n+m
Overall elongation ratio ($\Delta\mu / L$)	1
Overall twist curvature ($\Delta\phi / L$)	1
summation	5 n+5 m+1

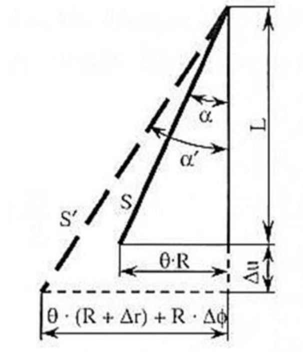

Fig. 2 The geometry of helical tendon before and after deformation

2.1 Helical layers

Deploy a helical tendon to a line. The geometric relationship of the helical tendon before and after deformation can be represented as Fig. 2.

According to Fig. 2, the axial strain can be expressed as

$$\varepsilon = \frac{S' - S}{S} \tag{1}$$

where S and S' represent the length of a helical tendon before and after deformation, which equals to

$$S = \frac{L}{\cos\alpha} \tag{2}$$

$$S = \frac{L + \Delta\mu}{\cos\alpha'} \tag{3}$$

where L and $\Delta\mu$ represent the length and elongation of the flexible riser; α and α' represent the lay angle of the helical tendon before and after deformation.

From Fig. 2, L and α' can be calculated from

$$L = \frac{R\theta}{\tan\alpha} \tag{4}$$

$$\cos\alpha' = \frac{L + \Delta\mu}{\sqrt{(L+\Delta\mu)^2 + [R\cdot\Delta\phi + (R+\Delta r)\theta]^2}} \tag{5}$$

In above two equations, R is the radius of the cylinder which is helically wound by the tendons, θ is circumferential angle that the helical tendon rotates; Δr and $\Delta\phi$ represent variances in the radius and circumferential angle, separately.

According to the first assumption, the riser deforms with small strain and small displacement. Combining Eqs. (4) and (5) along with Eqs. (2) and (3), and substituting the results into Eq. (1), the axial strain of a helical tendon can be derived, in which high order infinitesimal is neglected

$$\varepsilon = \cos^2\alpha \cdot \frac{\Delta\mu}{L} + R\cdot\sin\alpha\cos\alpha\cdot\frac{\Delta\phi}{L} + \sin^2\alpha\cdot\frac{\Delta r}{R} \tag{6}$$

Based on constitutive equation, the axial force of a helical tendon can be expressed as

$$F = EA\cdot\varepsilon = EA\cdot(\cos^2\alpha\cdot\frac{\Delta\mu}{L} + R\cdot\sin\alpha\cos\alpha\cdot\frac{\Delta\phi}{L} + \sin^2\alpha\cdot\frac{\Delta r}{R}) \tag{7}$$

where E and A are the Young's modulus and the cross-sectional area of the tendon.

As shown in Fig. 2, the tangential line of the helical tendon forms an intersection angle α with the axis of the flexible riser. Projecting the axial force of helical tendons into the axis of the riser and considering the quantity of helical tendons, the contribution of tendon layers to the axial force of the riser can be derived as

$$F_i = n_i\cdot F\cdot\cos\alpha = n_i\cdot EA\cdot(\cos^3\alpha\cdot\frac{\Delta\mu}{L} + R\cdot\sin\alpha\cos^2\alpha\cdot\frac{\Delta\phi}{L} + \sin^2\alpha\cos\alpha\cdot\frac{\Delta r}{R}) \tag{8}$$

Similarly, projecting the axial force of helical tendons into the circumfrencial direction of the tendon layer and taking radius R into account, the contribution of tendon layers to the torque of the riser can be deduced as

$$M_{t,i} = n_i\cdot F\cdot\sin\alpha\cdot R = n_i\cdot EA\cdot R\cdot(\cos^2\alpha\sin\alpha\cdot\frac{\Delta\mu}{L} + R\cdot\sin^2\alpha\cos\alpha\cdot\frac{\Delta\phi}{L} + \sin^3\alpha\cdot\frac{\Delta r}{R}) \tag{9}$$

When helical tendons deform and contact adjacent layers, the contact pressure can be generated as Ramos Jr. (2004)

$$P_{c,i-1} - P_{c,i} = \frac{\sin^2\alpha}{R\cdot b}\cdot EA\cdot(\cos^2\alpha\cdot\frac{\Delta\mu}{L} + R\cdot\sin\alpha\cos\alpha\cdot\frac{\Delta\phi}{L} + \sin^2\alpha\cdot\frac{\Delta r}{R}) \tag{10}$$

where, $P_{c,i-1}$ represents the contact pressure between the helical layer and the adjacent layer inside; $P_{c,i}$ represents the contact pressure between the helical layer and the adjacent layer outside; b is the thickness of the helical layer.

On the basis of the constitutive equation, the variance in thickness of helical tendons caused by axisymmetric force can be written as

$$\Delta t = -\frac{t}{2E}\cdot(P_{c,i-1} + P_{c,i}) - \nu\cdot t\cdot\cos^2\alpha\cdot\frac{\Delta\mu}{L} - \nu\cdot t\cdot R\cdot\sin\alpha\cos\alpha\cdot\frac{\Delta\phi}{L} - \nu\cdot t\cdot\sin^2\alpha\cdot\frac{\Delta r}{R} \tag{11}$$

For an unbonded flexible riser with n helical layers, Eqs. (8)-(11) can provide 4n Eqs. for the sets of Eqs., by which the axisymmetric response of the flexible riser can be analyzed.

2.2 Cylindrical layers

According to thick wall cylinder theory, the axial strain ε_z, circumferential strain ε_θ, radial strain ε_r, axial stress σ_θ and radial stress σ_r in the cylindrical layer can be written as

$$\varepsilon_z = \frac{\Delta\mu}{L} \tag{12}$$

$$\varepsilon_\theta = \frac{\Delta r}{R} \tag{13}$$

$$\varepsilon_r = \frac{d\Delta r}{dR} = \frac{\Delta t}{t} \tag{14}$$

$$\sigma_\theta = \frac{P_i \cdot (R-t/2)^2 - P_0 \cdot (R+t/2)^2}{(R+t/2)^2 - (R-t/2)^2} + \frac{\left(P_i - P_0\right)\cdot (R-t/2)^2 \cdot (R+t/2)^2}{(R+t/2)^2 - (R-t/2)^2} \cdot \frac{1}{r^2} \tag{15}$$

$$\sigma_r = \frac{P_i \cdot (R-t/2)^2 - P_0 \cdot (R+t/2)^2}{(R+t/2)^2 - (R-t/2)^2} - \frac{\left(P_i - P_0\right)\cdot (R-t/2)^2 \cdot (R+t/2)^2}{(R+t/2)^2 - (R-t/2)^2} \cdot \frac{1}{r^2} \tag{16}$$

where, t and r in Eqs. (15) and (16) represent the thickness of the cylinder and the radius of a certain point in the cylinder cross section, separately.

According to constitutive Eqs., the axial force, torque, radial displacement and variance of the thickness can be written as

$$\begin{aligned} \frac{F}{A} &= \sigma_z = E \cdot \varepsilon_z + \nu \cdot \left(\sigma_r + \sigma_\theta\right) \\ &= (1-\frac{t}{2R}) \cdot \frac{\nu \cdot (2R-t) \cdot (P_i + \mu_{in} \cdot P_{in})}{2 \cdot t} - (1+\frac{t}{2R}) \\ &\quad \cdot \frac{\nu \cdot (2R+t) \cdot (P_o + \mu_o \cdot P_o)}{2 \cdot t} + E \cdot \frac{\Delta\mu}{L} \end{aligned} \tag{17}$$

$$M_t = GJ \cdot \frac{\Delta\phi}{L} \tag{18}$$

$$\begin{aligned} \Delta r &= \varepsilon_\theta \cdot R = \frac{R}{E} \cdot \left[\sigma_\theta - \nu \cdot \left(\sigma_r + \sigma_z\right)\right] \\ &= -\nu \cdot R \cdot \frac{\Delta\mu}{L} + (1-\frac{t}{2R}) \cdot \left[\frac{(1-\nu^2)\cdot R^2}{t \cdot E} + \frac{\nu \cdot (1+\nu) \cdot R}{2 \cdot E}\right] \cdot (P_i + \mu_{in} \cdot P_{in}) \\ &\quad - (1+\frac{t}{2R}) \cdot \left[\frac{(1-\nu^2)\cdot R^2}{t \cdot E} - \frac{\nu \cdot (1+\nu) \cdot R}{2 \cdot E}\right] \cdot (P_o + \mu_o \cdot P_o) \end{aligned} \tag{19}$$

$$\begin{aligned} \Delta t &= \varepsilon_r \cdot t = \frac{t}{E}\left[\sigma_r - \nu \cdot \left(\sigma_\theta + \sigma_z\right)\right] \\ &= -\nu \cdot t \cdot \frac{\Delta\mu}{L} + (1-\frac{t}{2R}) \cdot \left[\frac{(1-\nu^2)\cdot t}{2 \cdot E} + \frac{\nu \cdot (1+\nu) \cdot R}{E}\right] \cdot (P_i + \mu_{in} \cdot P_{in}) \\ &\quad - (1+\frac{t}{2R}) \cdot \left[\frac{(1-\nu^2)\cdot t}{2 \cdot E} - \frac{\nu \cdot (1+\nu) \cdot R}{E}\right] \cdot (P_o + \mu_o \cdot P_o) \end{aligned} \tag{20}$$

Where, P_{in} and P_o are the inner and outer pressure that the flexible riser undergos, separately. μ_{in} and μ_o in the innermost and outermost cylindrical layer equal to 1, while, the two parameters in other layers equal to 0.

For an unbonded flexible riser with m cylindrical layers, 4 m equations, shown in Eqs. (17)-(20) can help to predict the structural response of the flexible riser.

2.3 Overall layers

Radius relationship of the adjacent layers in the flexible riser can be written as

$$\Delta R_{i+1} = \Delta R_i + \frac{1}{2} \cdot (\Delta t_{i+1} + \Delta t_t) + g_i \qquad 1 \leq i \leq n+m-1 \tag{21}$$

where， g_i is the interlayer gap.

According to the equilibrium in the whole riser, the summation of the axial forces, which each layer withstand, equals to the axial force of the whole riser. This is the same with the torque. The equilibrium relations can be expressed as

$$F = \sum_{i=1}^{n+m} F_i \tag{22}$$

$$M_t = \sum_{i=1}^{n+m} M_t \tag{23}$$

Therefore，5n+5m+1 unknown variables listed in Table1 can be solved by 5n+5m+1 linear equations, which are consist with Eqs. (8), (9), (10), (11), (17), (18), (19), (20), (21), (22) and (23). The axisymmetric response in each layer can hence be predicted.

3. Finite element model

Witz (1996) published a case study in structural analysis of a 2.5-inch unbonded flexible riser. Both construction details and experimental results for axisymmetric and bending behavior are provided. This 2.5-inch unbonded flexible riser has been chosen here as the study case to develop the finite-element model. Detailed information on the flexible riser is listed in Table 2.

A detailed finite-element model with 1.288m in length is developed as shown in Fig. 2. The model consists of eight separate layers. In particular, the carcass layer and the zeta layer are modeled in a more realistic and detailed way than the models in Refs. (Zhang and Tuohy 2002, Bahtui and Bahai 2008a,b).

All layers in this model are modeled by 3D, eight-node linear brick, reduced integration elements, which enables much more accurate contact analysis. Contact elements are defined between each layer, and the contact analysis is based on the Coulomb friction model together with the general contact algorithm. The frictional coefficient between layers is assumed to be 0.1, as given by experimental results in Ref. (Saevik and Berge 1995). A well-distributed mesh containing 677,262 elements and 286,472 nodes is used to keep the artificial energy well below 5% of the strain energy.

The ends of all layers are connected rigidly to two reference nodes at the center of each cross section. All boundary conditions for both ends are then applied to these two reference nodes only.

Table 2 Geometric and material parameters of the flexible riser

Layer	**Modulus (Mpa)**	**Inner radius (mm)**	**Thickness (mm)**	**Lay angle (°)**	**Number of helical tendons**
Carcass	1.9E5	63.2	3.5	87.5	1
Inner sheath	2.84E2	70.2	4.9	–	–
Compressive layer	2.07E5	80.1	6.2	85.5	1
First anti-wear layer	3.01E2	92.5	1.5	–	–
First tensile layer	2.07E5	95.5	3.0	35 (clockwise)	40
Second anti-wear layer	3.01E2	101.5	1.5	–	–
Second tensile layer	2.07E5	104.5	3.0	35(counterclockwise)	44
Outer sheath	Axial stiffness 600 transverse stiffness 300	110.5	0.5	–	–

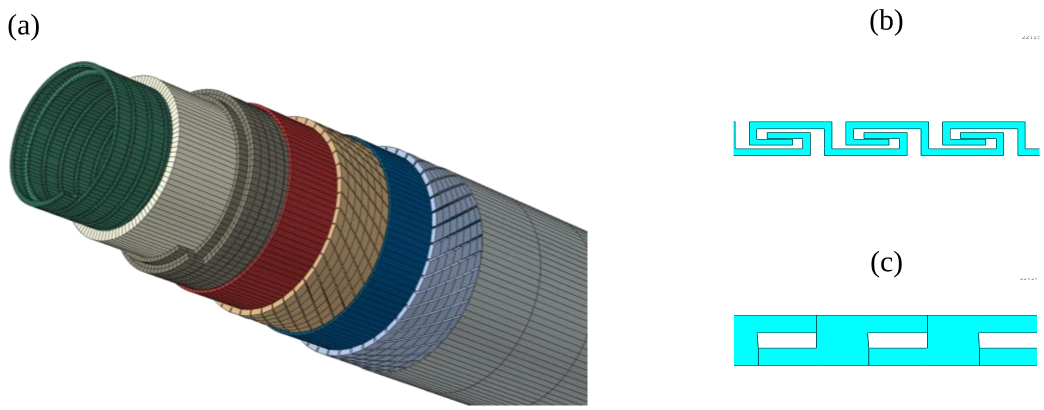

Fig. 2 Finite-element model of the flexible riser: (a) whole model, (b) carcass layer profile and (c) zeta layer profile

4. Results analysis

Based on the developed analytical model and the numerical model in this paper, the structural behavior of the flexible riser under axisymmetric loads can be predicted. The comparison of the results with experimental data obtained from the literature (Witz 1996) is shown in the following figures.

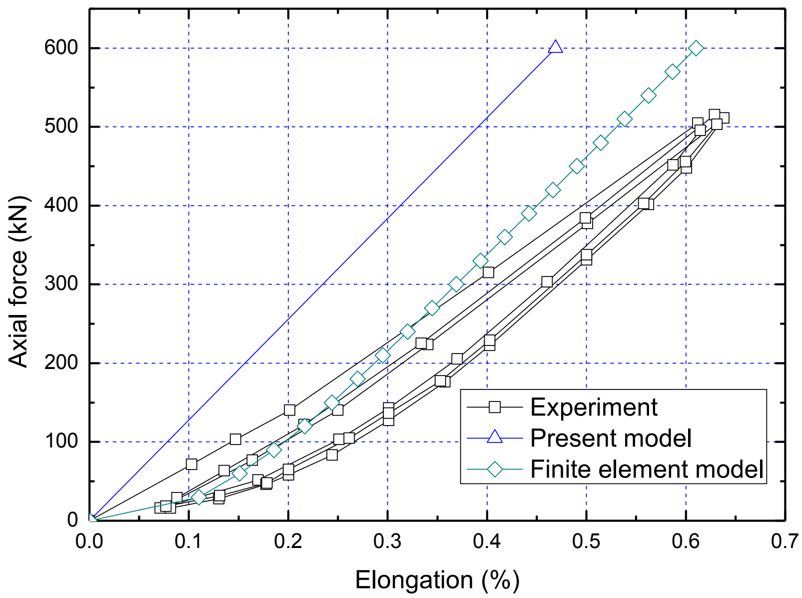

Fig. 3 Axial force-elongation relationship of the flexible riser with ends free to rotate

The experimental structural behavior for the flexible riser under tension with ends free to rotate (Witz 1996) is presented as the hysteric curve in Fig. 3. The measured axial force-elongation curve shows slightly non-linear behavior with hysteresis characteristics, and the measurement clearly shows that the riser is becoming stiffer with increasing elongation. This is mainly due to the fact that interlayer gaps exist between adjacent layers in the flexible riser. These gaps influence the interaction of the layers and thus introduce non-linearity in the axial behavior. When the load is acting on the flexible riser in the first stage, the radial support is not obvious because of the gaps between layers. Main strong components, such as tensile layers, display relatively large radial displacement, which lowers the axial stiffness of the flexible riser. With increase in the tension load, all the layers contact tightly together. Then, the radial displacement of the tensile layer dwindles, and the tensile stiffness increases until reaching a steady state.

The analytical and numerical results for the same riser under tension load are also presented in Fig. 3. Linear behavior can be observed from the analytical results, however, non-linear behavior are shown in the numerical result. Comparing the analytical and experimental stiffness, good agreement can be found when elongation is relatively high, while obvious difference is presented when elongation is low. This phenomenon chiefly owes to the assumption that no initial gap exists in the analytical model in this paper. The analytical results are consistent with experimental data after the gaps between layers are closed.

Compared with the analytical model, the numerical model can capture the non-linear behavior of axial force-elongation relationship well. This is due to the fact that the increase in radial support between adjacent layers with the increasing of the tension load can be accurately simulated. Comparing the numerical results with experimental ones, the numerical result shows satisfactory agreement with the experimental result.

Table 3 Results comparison for tensile response of the flexible riser with ends free to rotate

	(N/ε) / MN	$(\Delta\phi/\varepsilon)$ / (rad/m)
Average value of results of institution models	128	-1.86
Experimental data	36~138	-
Result of analytical model	129	-1.5
Result of FEM	27~122	-

Because of the helical configuration of the tendons, the flexible riser is inclined to rotate under tension loads alone. The coupled rotation deformation can also be predicted by the analytical model, which is listed in Table 3. Besides, the comparisons of tensile stiffness between presented models in this paper and models established by institutions (Witz 1996) are also shown in Table 3.

From the comparisons in Fig. 3 and Table 3, reasonable agreements have been found among the analytical, numerical and experimental results, which illustrates the reliability and correctness of the analytical and numerical models developed in this paper.

Under torsional loading, the comparison of the structural response is presented in Fig. 4.

The experimental structural behavior for the flexible riser under torsion with ends fixed axially (Witz 1996) is presented as the hysteric curve in Fig. 4. The measured axial torque-twist curve shows slightly non-linear behavior with hysteresis characteristics, the reason for this fact is the same as that for the tension result in Fig. 3. Comparing the torsional stiffness of the flexible riser under torsion in clockwise and anticlockwise direction, much difference can be found in the results. When the load is acting anticlockwise, outer tensile layer is in the tension state. The tendon tightens up and a high torsional stiffness is induced. When the load is in clockwise direction, the outer tensile layer is compressed and gaps emerge between adjacent layers. In this case, low torisonal stiffness is expected.

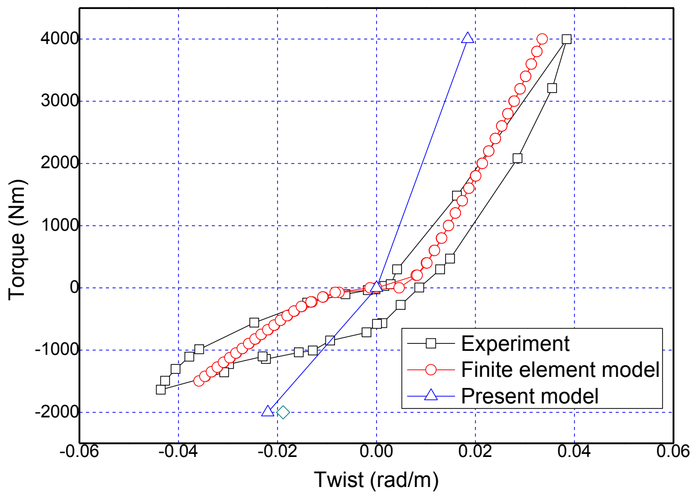

Fig. 4 Torque-twist relationship of the flexible riser with ends fixed axially

Table 4 Results comparison for twist response of the flexible riser with ends fixed axially

	Clockwise		Anticlockwise	
	(M/ϕ) / (kNm^2/rad)	(N/ϕ) / (MNm/rad)	(M/ϕ) / (kNm^2/rad)	(N/ϕ) / (kNm/rad)
Average value of results of institution models	106	-1.77	203	597
Experimental data	17~62	-	95~152	-
Result of analytical model	91	-2.17	217	473
Result of FEM	17~60	-	40~158	-

Table 5 Table 4 Results comparison for twist response of the flexible riser with ends free to elongation

	Clockwise		Anticlockwise	
	(M/ϕ) / (kNm^2/rad)	(ε/ϕ) / (mm/rad)	(M/ϕ) / (kNm^2/rad)	(ε/ϕ) / (mm/rad)
Average value of results of institution models	28	26.5	174	-93
Result of analytical model	28	28.4	177	-143

The analytical and numerical results for the riser under torsion are also are presented in Fig. 4. Linear behavior can be observed from the analytical results, however, non-linear behavior are shown in the numerical result. Comparing the analytical and experimental results, the torsional stiffness computed theoretically is larger than that measured in the experiments. This is probably due to several assumptions, such as the assumption of the uniform variance in radius and thickness in each layer, are not satisfied in experimental test. Observing the results of analytical stiffness in different directions, the presented analytical model can capture the impact of the torque's load directions on the torsional stiffness. Compared with the analytical model, the numerical results behave non-linearly and agree well with the experimental data.

The results of torque response of the flexible riser with different boundary conditions are listed in Tables 4 and 5.

From comparisons of the results in Fig. 4, Tables 4 and 5, it can be found that the analytical model and numerical model presented in this paper can provide a good prediction on the torque response for the flexible riser.

The analytical torsional stiffness with ends prevented from elongation in Table 3 is much larger than the corresponding results in Table 4. This fact illustrates that the coupled interaction between axial elongation and torsional deformation has a great effect on the torsional stiffness, to which special attention should be paid in the analysis and design of the flexible riser.

Based on the analytical model presented in this paper, the structural response under other kinds of axisymmetric loads is listed in Table 6.

Table 6 Response results of the flexible riser under other axisymmetric loads

Loading type	parameter	result
Compression(with ends free to rotate)	(N/ε) / (MN)	4.2
	($\Delta\phi/\varepsilon$) / (rad/m)	14.92
Internal pressure (with ends free to rotate and elongation)	(P/ε) / (MPa)	-1.3E5
	($\Delta\phi/\varepsilon$) / (rad/m)	25.4
External pressure(with ends free to rotate and elongation)	(P/ε) / (MPa)	1.4E4
	($\Delta\phi/\varepsilon$) / (rad/m)	4.6

Table 6 shows that the analytical model presented in this paper can predict the structural response to all kinds of axisymmetric loads. Compressive stiffness is smaller than tensile stiffness. This is mainly due to the fact that fairly large radial displacement occurs under compression, which lowers the axial stiffness of the flexible riser.

5. Conclusions

Based on equilibrium conditions, geometrical relations and the constitutive equations, the analytical model that can accurately predict the axisymmetric behavior of the flexible riser is deduced in this paper. Meanwhile, a detailed numerical model is also developed. With the analytical and the numerical model, response of the flexible riser under tension, torsion as well as internal and external pressure is computed and compared with experimental results obtained from literature. The following conclusions are drawn:

- The analytical model and the numerical model in this paper can effective predict axisymmetric response of flexible risers, and provide an effective approach for designing flexible risers.
- Initial interlayer gaps and friction are main factors to account for nonlinearity in the axisymmetric response of flexible risers.
- The laying configuration of helical tendons results in the coupling effect between tension and twist. The coupling effect leads to big difference in axisymmetric stiffness of the flexible riser under different boundary conditions.
- Different interlayer gaps emerge due to loads in various directions, as a result, the structural response of flexible risers also behaves differently.
- The FE model presented in this paper has the potential to be employed in the more complex failure modes such as lateral buckling. However, in order to deal with the buckling failure, the material nonlinear has to been incorporated.
- Experimental data are not widely available in literature to validate analytical results. More experimental investigating is recommended to conducted and published.

References

Bahtui, A., Bahai, H. and Alfano, G.A. (2008a), "Finite element analysis for unbonded flexible risers under axial tension", *Proceedings of the 27th International Conference on Offshore Mechanics and Arctic Engineering*, Estoril.

Bahtui, A., Bahai, H. and Alfano, G.A. (2008b), "Finite element analysis for unbonded flexible risers under torsion", *J. Offshore Mech. Arct*., **130**(4), 041301.

Claydon, P., Cook, G., Brown, P. *et al.* (1992), "A theoretical approach to prediction of service life of unbonded flexible risers under dynamic loading conditions", *Mar. Struct*., **5**(5), 399-429.

Do, K.D. (2011), "Global stabilization of three-dimensional flexible marine risers by boundary control", *Ocean Syst. Eng*., **1**(2), 171-194.

Feret, J.J. and Bournazel, C.L. (1987), "Calculation of stresses and slip in structural layers of unbonded flexible risers", *J. Offshore Mech. Arct*.**,** **109**(3), 263-269.

Huang, H., Zhang, J. and Zhu, L. (2013), "Numerical model of a tensioner system and riser guide", *Ocean Syst. Eng*., **3**(4), 257-273.

Lanteigne, J. (1985), "Theoretical estimation of the response of helically armored cables to tension, torsion, and bending", *J. Appl. Mech. -T ASME*, **52**, 423-432.

Mcnamara, J.F. and Harte, AM. (1989), "Three dimensional analytical simulation of flexible pipe wall structure", *Proceedings of the 8th International Conference on Offshore Mechanics and Arctic Engineering*.

Ramos R., Jr. and Pesce, C.P.A. (2004), "Consistent analytical model to predict the structural behavior of flexible risers subjected to combined loads", *J. Offshore Mech. Arct.*, **126**(2), 141-146.

Saevik, S. and Berge, S. (1995), "Fatigue testing and theoretical studies of two4 in flexible pipes", *Eng. Struct*., **17**(4), 276-292.

Saevik, S. and Bruaseth, S. (2005), "Theoretical and experimental studies of the axisymmetric behaviour of complex umbilical cross-sections", *J. Appl. Ocean Res*., **27**(2), 97-106.

Witz, J.A. and Tan, Z. (1992), "On the axial-torsional structural behaviour of flexible risers", *J. Umbilicals Marine Cables Marine Struct*., **5**(2-3), 205-227.

Witz, J.A.A. (1996), "Case study in the cross-section analysis of flexible risers", *Mar. Struct*., **9**(9), 885-904.

Zhang, W. and Tuohy, J. (2002), "Application of finite element modelling in the qualification of large diameter unbonded flexible risers", *Proceedings of the 21st International Conference on Offshore Mechanics and Arctic Engineering*, Oslo.

Zou, J. (2011), "Semisubmersible platforms with Steel Catenary Risers for Western Australia and Gulf of Mexico", *Ocean Syst. Eng*., **2**(2), 99-113.